Received: 5 August 2016 | Revised: 23 November 2016 | Accepted: 3 January 2017

DOI: 10.1002/jemt.22840

RESEARCH ARTICLE

WILEY

Zinc oxide 3D microstructures as an antimicrobial filler content for composite resins

Hércules Bezerra Dias[1,2] | Maria Inês Basso Bernardi[2] | Matheus Aparecido dos Santos Ramos[3] | Tamara Carolina Trevisan[1] | Taís Maria Bauab[3] | Antônio Carlos Hernandes[2] | Alessandra Nara de Souza Rastelli[1]

[1]Department of Restorative Dentistry, Araraquara School of Dentistry, São Paulo State University - UNESP, Araraquara, SP, 14801-903, Brazil

[2]Physics Institute of São Carlos - IFSC, University of São - USP, São Paulo, São Carlos, SP, 13566-590, Brazil

[3]Department of Biological Sciences, School of Pharmaceutical Sciences, São Paulo State University - UNESP, Araraquara, SP, 14801-902, Brazil

Correspondence
Prof. Dr. Alessandra Nara de Souza Rastelli, São Paulo State University - UNESP, Araraquara School of Dentistry, Department of Restorative Dentistry, Araraquara, SP, Brazil
Email: alrastelli@foar.unesp.br

Funding information
The Amazon State Research Foundation (FAPEAM, AM, Brazil) and Coordination for the Improvement of Higher Education Personnel (CAPES, Brazil)

Abstract

The aim of this study was to evaluate the antibacterial activity of a composite resin modified by 3D zinc oxide (ZnO) microstructures and to verify possible alterations on its mechanical properties. ZnO was synthesized by hydrothermal approach and characterized by X-ray diffraction (XRD), surface area by Brunauer, Emmett and Teller (BET), Fourier transform infrared spectroscopy (FTIR) and Field emission scanning electron microscopy (FESEM). The minimum inhibitory concentrations of ZnO against *Streptococcus mutans*, *Escherichia coli*, *Staphylococcus aureus*, and *Candida albicans* were determinated. The composite resin Filtek™ Z350XT (3M of Brazil) was blended with 0.2%, 0.5%, and 1% in weight of ZnO and submitted to antibacterial assay by direct contact test against *S. mutans*, the leading cause of dental caries and the most cariogenic oral streptococci. Additionally, it was performed compressive and diametral tensile strength tests of the modified composite resin. Microrods and hollow microrods of ZnO were obtained and its MIC values were found to be 125 μg/mL for *S. mutans*, 500 μg/mL for *C. albicans* and 62.5 μg/mL for *S. aureus*. For the tested concentrations, it was not found MIC against *E. coli*. The direct contact test showed a significant antibacterial capacity of modified composite resin ($p > 0.05$ for all concentrations). The compressive and diametral tensile strength remains no changed after inclusion of microparticles ($p > 0.05$ for all concentrations). The modification of the composite resin with small amounts of ZnO microparticles significantly inhibited the *S. mutans* growth on resin surface without significant alterations of its mechanical strength.

KEYWORDS
composite resins, oxides, products with antimicrobial action, *Streptococcus mutans*

1 | INTRODUCTION

The main cause of secondary caries is the accumulation of dental plaque on the surface of dental restorative materials, resulting in the need of replacement of restorations (Burke et al., 2001; Sakaguchi, 2005). The use of nano and microparticles to modify dental restorative materials have been grown and researches are focused in development of a restorative material resistant to bacterial accumulation (Gjorgievska et al., 2015; Corrêa et al., 2015). The incorporation of metal oxides is one of the approaches that have been used to achieve antibacterial activity into the resin-based restorative materials (Wang, Shen, & Haapasalo, 2014). It was previously demonstrated that nanoparticles of zinc oxide (ZnO) have a broad antimicrobial spectrum (Raghupathi, Koodali, & Manna, 2011), and they have been used successfully to modify resin based restorative materials, leading to a reducing of bacterial biofilms on the surface of this materials (Hojati et al., 2013; Kasraei et al., 2014; Sevinç et al., 2011). This high antimicrobial capacity could be attributed to their size and high surface area. However, smallness in itself is not the goal, the use of different methods of synthesis in order to obtain novel physicochemical properties are also relevant variables affecting antibacterial activity (Pal, Tak, & Song, 2007; Seil & Webster, 2012). The shape of particles have been described as an important role in the reactive oxygen species production and antibacterial activity (Pal, Tak, & Song, 2007; Seil & Webster,

2012; Sirelkhatim et al., 2015; Yang, Liu, Yang, Zhang, & Xi, 2009). In this way, the rods and wires of ZnO have demonstrated better results than spherical particles (Sirelkhatim et al., 2015; Yang, Liu, Yang, Zhang, & Xi, 2009). The antibacterial activity of different shapes of ZnO, such as nanorods, microrods, nanospheres, microspheres, and microflowers, have been reported (Rago et al., 2014; Wahab, Kim, Mishra, Yun, & Shin, 2010; Wahab et al., 2012). Since ZnO presents a wide range of shapes (Raghupathi et al., 2001; Sahu, Liu, Wang, & Kuo, 2015) and its antibacterial capacity is shape-dependent (Pal, Tak, & Song, 2007), ZnO morphology has become a determinant factor in the choice of this material in nano and microscale to modify composite resins. This can be achieved by controlling of parameters such as pH, temperature, solvents, precursor types and physicochemical settings of synthesis (Sirelkhatim et al., 2015). Although the incorporation of ZnO in composite resin can impart antibacterial activity, physical and mechanical properties can be drastically affected and this should be controlled taking into consideration the size, quantity, color, and opacity of particles (Powers, 2006).

Since the physical parameters of particles are directly related to their properties and can influence the particle-microorganism interaction, it is interesting to analyze the properties of a composite resin modified by ZnO microstructures with three dimensional morphology and controlled chemical-physical characteristics. In this way, the aim of this study was to synthesize and characterize microrods and hollow microrods of ZnO, insert it into a composite resin and evaluate its mechanical and antibacterial properties in order to obtain a novel restorative material with antibacterial capacity, increasing the longevity of restorations and its clinical acceptance. The null hypotheses tested were: (1) There is no difference on antibacterial capacity of a composite resin after its modification with ZnO microstructures. (2) There is no difference on compressive and diametral tensile strength of a composite resin after its modification with ZnO microstructures.

2 | MATERIALS E METHODS

2.1 | Experimental design

This is an experimental study, which have dependent variables (compressive strength, diametral tensile strength and antibacterial capacity (CFU/mL) and independent variables [ZnO concentrations (wt%)].

2.2 | Synthesis of ZnO hexagonal microrod-like structures by hydrothermal approach

ZnO hexagonal microrod-like and hollow microrod-like structures were prepared by dissolving equimolar (0.1 mol·L^{-1}) zinc nitrate [$Zn(NO_3)_2{\cdot}6H_2O$, Aldrich, >99%] and hexamethylenetetramine (HMTA, $C_6H_{12}N_4$, Aldrich, >99%) in deionized water (Jabeen, Iqbal, Kumar, Ahmed, & Javed, 2014). The resultant solution was placed in a borosilicate glass bottle (BOECO Germany) with a screw cap. This glass bottle was placed in a furnace for 6 hr at 110°C. The resultant white precipitate was collected by centrifugation, washed several times with deionized water and alcohol isopropyl, and dried at 80°C for 12 hr in an air atmosphere.

2.3 | Characterization of ZnO microparticles

X-Ray diffraction (XRD) patterns of the ZnO powder were recorded on a Rigaku, Rotaflex RU200B diffraction system with high intensity Cu Kα radiation (λ = 1.5406 Á), at 25°C with 2θ values ranging from 20 to 80°C and scanning rate of 0.02°C per min. The crystallite size was determined by Scherrer equation ($D = K\lambda/(\beta \cos \theta)$ where λ is the wavelength of the X-ray radiation, K is a constant taken as 0.89, θ is the diffraction angle, and β is the full width at half maximum (FWHM)) (Alexander & Klug, 1950).

The FTIR measurements of ZnO particles were carried out in the Nexus 670 FTIR spectrophotometer (Thermo Scientific, Madison, WI). A total of 64 scans were collected from 4000 to 650 cm^{-1} at 4 cm^{-1} resolution. Nitrogen adsorption–desorption measurements for the products were performed using a Micromeritics ASAP 2020 M + C instrument using Barrett–Emmett–Teller calculations for surface area determination. The isotherms and hysteresis curves were classified according to IUPAC (*International Union of Pure and Applied Chemistry*). The particle size (D_{BET}) was calculated using the following equation:

$$D_{BET} = \frac{6}{A_s \cdot \rho}$$

where A_s is the superficial area (m^2/g) and ρ is the density of material (ZnO = 5.675 JCPDF 36-1451).

Field emission scanning electron microscopy (FESEM) analysis of ZnO powder was carried out on a high resolution scanning electron microscopy (FESEM Supra 35, Zeiss, Germany) operating at 3 kV.

2.4 | In vitro evaluation of antimicrobial activity of ZnO microstructures

2.4.1 | Antibacterial assay

2.4.1.1 | Microorganisms and preparation of bacterial suspensions

It was used the following bacterial strains: *Escherichia coli* (ATCC 25922), *Staphylococcus aureus* (ATCC 25923) and *Streptococcus mutans* (ATCC 25175). All strains were purchased from American Type Culture Collection. A suspension of *S. mutans* was prepared in Brain Heart Infusion Broth (BHIB) and incubated (37°C in 10% CO_2 atmosphere) for 24 hr, while *E. coli* and *S. aureus* were prepared in Mueller Hinton broth (MHB) at 37°C for 24 hr. They were transferred to culture medium sterile and diluted to a 0.5 McFarland scale (10^8 CFU/mL). These suspensions were diluted (1/10) to obtain 10^7 CFU/mL, the final concentration used in the experiments (Araújo et al., 2012).

2.4.1.2 | Determination of the minimum inhibitory concentration (MIC)

The evaluation of the antibacterial activity and MIC determination were carried out by microdilution technique according to the methodology described by document M7-A6 from Clinical and Laboratory Standards Institute (CLSI) (CLSI, 2006), with modifications. It was added

TABLE 1 Composite resin used in this study

Nanohybrid CR	Manufacturer	Resin matrix	Filler	Filler, weight/volume
Filtek Z350 XT	3M Brazil	TEGDMA, UDMA, BIS–EMA	Combination of nonaggregated 20 nm silica, nanoaggregated 4-11 nm zirconia, and aggregated zirconia/silica cluster filler	78.5/59.5

CR, Composite resin; UDMA, Urethane dimethacrylate; BIS–EMA, Bisphenol A ethoxylated dimethacrylate; TEGDMA, Triethylene glycoldimethacrylate.

(80 μL) in each well of the microplate (96 wells) MHB to *E. coli* and *S. aureus* and BHIB to *S. mutans*. ZnO microparticles were suspended in distilled water (2000 μg/mL) and it was added 100 μL of this suspension in each well of microplate, and then the serial dilutions were carried out from 1000 to 7.8 μg/mL. After that, 20 μL of suspensions of microorganism was distributed in each well of the microplate. As positive control was used ampicilin (100 to 0.3 μg/mL). It was also performed the control of the medium, the bacterial growth, and sterility of solvent (distilled water). The microplates with *E. coli* and *S. aureus* were incubated at 37°C for 24 hr, while *S. mutans* was incubated at 37°C in a 10% CO_2 atmosphere for 24 hr.

2.4.1.3 | Readings

After the incubation period, 30 μL of an aqueous solution (0.01%) of resazurin was add, and incubated at 37°C for 2 hr. The absence of growth of the bacteria maintains the solutions of the wells in blue, while the pink color represents the microorganism growth (Araújo et al., 2012). Additionally, spectrophotometric readings (microplate reader EPOCH 2) (595 nm) were carried to obtain the percentage inhibition of each compound against microorganisms. The MIC value was defined as the concentration capable of inhibiting ≥90% of bacterial growth (Gudiña, Rocha, Teixeira, & Rodrigues, 2010).

2.4.2 | Antifungal assay

2.4.2.1 | Preparation of fungal suspension

A fungal strain of *Candida albicans* (ATCC 10231) was used. After growth of *C. Albicans* in Sabouraud Dextrose Agar (SDA), the suspension was diluted in sterile PBS to obtain a 0.5 McFarland scale (10^6 CFU/mL) by spectrophotometric reading at 530 nm and counting in a Neubauer chamber. This suspension was diluted (1/1000) to obtain 10^3 CFU/mL, the final concentration used in the experiments (Bonifácio et al., 2015).

2.4.2.2 | Determination of the minimum inhibitory concentration (MIC)

The evaluation of the antifungal activity and MIC determination were carried out by microdilution technique according to the methodology described by document M27-A3 from Clinical and Laboratory Standards Institute (CLSI) (CLSI, 2008), with modifications. It was added (100 μL) in each well of the microplate (96 wells) Roswell Park Memorial Institute culture medium (RPMI) 1640 with MOPS (3-[*N*-morpholino] propanesulfonic) at pH 7.0. It was also added 100 μL in each of the ZnO microparticles suspension (2000 μg/mL) then, the serial dilutions were carried out from 1000 to 7.8 μg/mL. After, 100 μL of suspensions of microorganism was distributed in each well of the microplate. Amphotericin B (16.0–0.06 μg/mL) and fluconazole (512–1.0 μg/mL) were used as positive control. It was also performed the control of the medium, the yeast growth, and sterility of solvent. The microplate was incubated at 37°C for 48 hr.

2.4.2.3 | Readings

After incubation period, 20 μL of an aqueous solution of 2% 2,3,5-triphenyltetrazolium chloride (TTC) were added and the microplates were incubated at 37°C for 3 hr. The absence of growth of the microorganism maintains the colorless solutions of wells, while the red color represents the microorganism growth (Araújo et al., 2013). Additionally, spectrophotometric readings (595 nm) were carried to obtain the percentage inhibition of each compound against microorganisms. The MIC value was defined as the concentration capable of inhibiting ≥90% of bacterial growth (Bonifácio et al., 2015).

2.5 | Composite resin used in this study

The nanohybrid composite resin Filtek™ Z350XT (3M Brazil) at color A_2B (Body), employed as a control group and modified by ZnO microparticles for experimental groups was used. A summarized composition of this composite resin is showed in Table 1.

2.6 | Composite resin modification and preparation of test specimens

ZnO microparticles were added into the composite resin Filtek™ Z350XT (3M Brazil) using a standardized protocol based on the inclusion of weight percentage of particles into the composite resin (Das Neves, Agnelli, Kurachi, & de Souza, 2014). After weighed of microparticles corresponding to 0.2, 0.5, and 1% (wt%), these amounts were incorporated into the resin by manual mixing for 1 min, using a metal spatula and a glass plate. The specimens were prepared immediately after resin modification. According to ANSI ADA specification n.27 (American National Standard, 1993), the resin specimens for compressive strength ($n = 32$) and diametral tensile strength ($n = 32$) were prepared using a stainless steel split molds (4 mm in diameter and 8 mm in height). Specimens for antibacterial test were prepared using a stainless steel mold (4 mm in diameter and 2 mm in height). The splits mold were placed on a glass slide and overfilled with the composite resin containing ZnO microstructures (0.2, 0.5, and 1% in weight). The holes of the mold were pressed with polyester strips and the top surface with another glass slide. For mechanicals tests, specimens were light

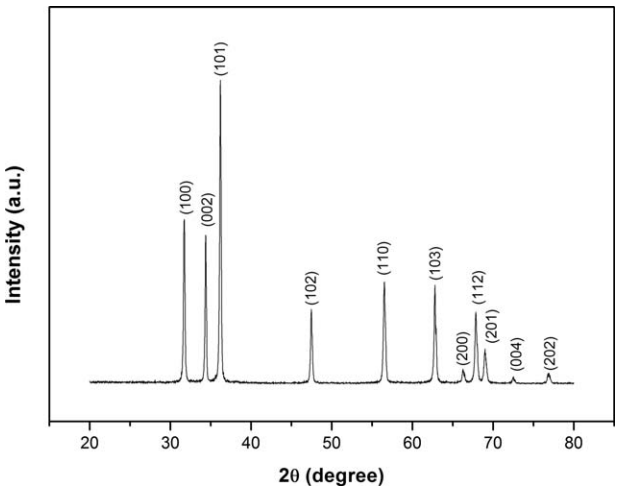

FIGURE 1 XRD pattern of ZnO synthesized by hydrothermal approach at 110°C for 6 hr

cured (LED Radii Plus - SDI, Australia) on top and bottom for 40s and after its removal from the mold, light cured in lateral for the same time. These specimens were stored in artificial saliva (Arte & Ciência, Araraquara, SP, Brazil, pH 7.0) and incubated (SPLabor, SP-200) at 37°C for 24 hr prior to test. For direct contact test, specimens were light-cured for 40s on the top and sterilized in an autoclave (120°C/15 min) prior the test.

2.7 | Antibacterial assay for composite resin modified by ZnO microstructures

2.7.1 | Direct contact test

Since *Streptococcus mutans* is the leading cause of dental caries worldwide and is considered to be the most cariogenic of all of the oral streptococci (Ajdic et al., 2002), this bacteria was the first choice to be used in this antibacterial assay. The composite resin modified by ZnO microstructures was tested by direct contact test (Kasraei et al., 2014). A suspension of *S. mutans* was prepared and standardized as previously described in this current study. The sterilized composite resins specimens were placed in a 24-well plate and then, 100 μL of bacterial suspension was placed on the surface of the specimens. They were incubated in an incubator at 37°C in 10% of CO_2 for 1 hr. After that, 900 μL of BHI broth plus 1% sucrose were added in each well and incubated at 37°C for 18 hr. The resultant suspensions of each well were submitted to tenfold several dilutions until 1:100,000. A micropipette was used to retrieve 25 μL from each tube to spread on brain-heart infusion agar (BHI Agar, HiMedia Laboratories Pvt. Ltd, India) plates, which was incubated at 37°C in 10% of CO_2 for 48 hr, and then the colony forming units (CFUs) were counted.

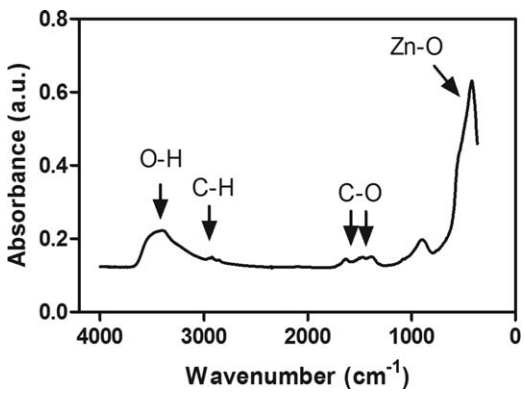

FIGURE 2 FTIR spectra of crystalline ZnO sample synthetized by hydrothermal approach at 110°C for 6 hr

2.8 | Compressive strength and diametral tensile strength tests

The compressive and diametral tensile strength tests were performed employing a mechanical test machine (DL2000, EMIC - Equipamentos e Sistemas de Ensaio Ltda., São José dos Pinhais, Paraná - Brazil) with a load cell of 5 KN at a cross-speed of 0.5 mm·min^{-1}. For compressive assessment, the specimens were placed with their flat ends between the plates of the testing machine and the compressive load was applied along the long axis of the specimens. For diametral tensile assessment, the specimens were compressed diametrically introducing tensile stress in the material. The fractured surface of resin specimens from mechanical test were submitted to FESEM (FESEM Supra 35, Zeiss, Germany) in backscattering electron mode and analyzed by energy dispersive X-ray spectroscopy (EDX) elemental composition (2.0×10^{-9} A, 30 kV, spot size of 500 nm, and 100 s).

2.9 | Statistical analysis

The data was analyzed using a GraphPad Prism 5 software. The normal distribution of the data was determined by Shapiro-Wilk test. One-way ANOVA and Tukey post hoc for multiple comparison were performed. The significance level was 5%.

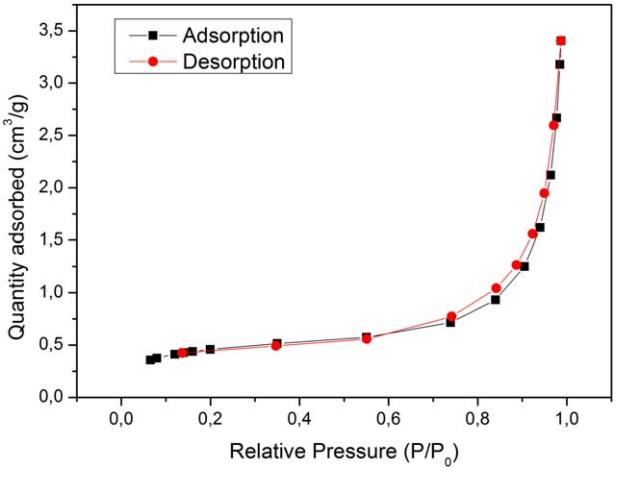

FIGURE 3 N_2 adsorption–desorption isotherms of ZnO powder synthesized by hydrothermal approach at 110°C for 6 hr. [Color figure can be viewed at wileyonlinelibrary.com]

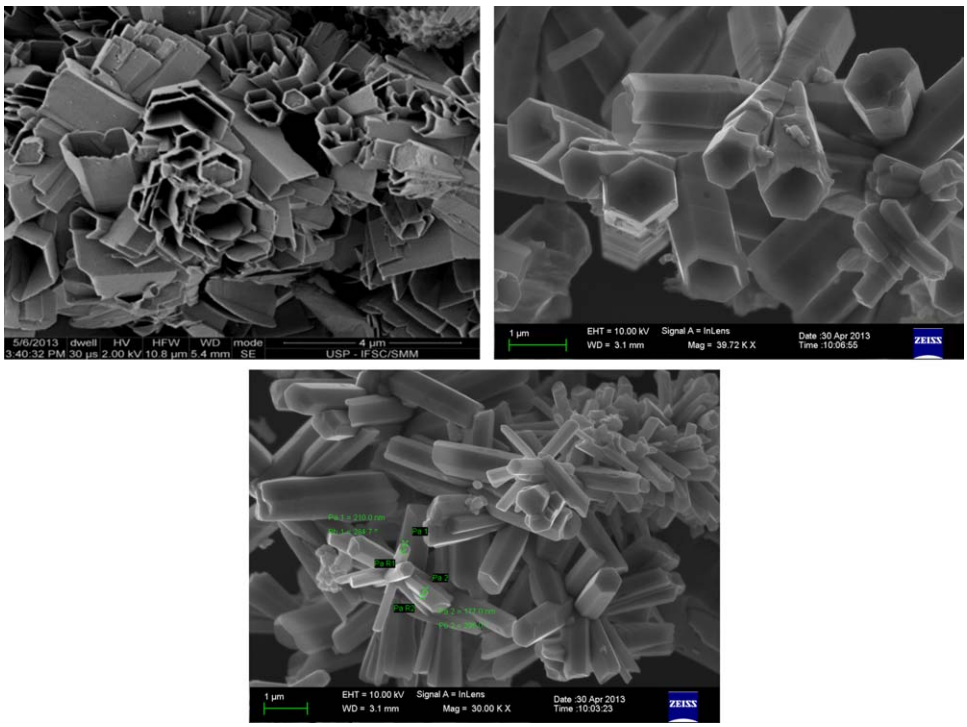

FIGURE 4 FESEM images of two microstructures founds on the same crystalline ZnO sample synthetized by hydrothermal approach at 110°C for 6 hr: Self-assembled microtubes (a) Type 1 (b) Type 2, and (c) Type 3. [Color figure can be viewed at wileyonlinelibrary.com]

3 | RESULTS

The crystal structure and phase composition of ZnO was revealed by XRD analysis. The typical pattern showed in Figure 1 is corresponding to crystalline ZnO powder and the diffraction peaks could be indexed to ZnO hexagonal wurtzite structure according to Joint Committee on Powder Diffraction Standards (JCPDS) file 36-1451. The crystallite sizes of the powders were estimated from X-ray line broadening using Scherrer's equation was found to be 42 nm.

The FTIR spectra of ZnO powder is showed in Figure 2. Typical infrared absorption spectra of ZnO synthesized by hydrothermal approach showed the strong absorption peaks at 435 cm^{-1} is the stretching mode ZnO. Moreover, it can be observed an absorption peak around 2,900, 1,450, and 1,380 cm^{-1} corresponds to C—H mode, C—OH in-off plane bending and C—OH.

The Figure 3 shows the N_2 adsorption–desorption isotherms of the crystalline ZnO powder. The isotherms shown are type IV with H1 hysteresis loops, characteristic of mesoporous materials with a narrow pore size distribution. According to IUPAC classification, based on diameter D of a solid, it can be classified as a microporous ($D < 20$ Å), mesoporous (20 Å $< D <$ 500 Å) or macroporous ($D >$ 500 Å).

FESEM images of ZnO powder prepared with Zinc Nitrate and HMTA, at 1:1 molar ratio by hydrothermal approach (110°C/6 hr), are showed in Figure 4. Different 3D morphologies were found for ZnO powder. It is clear in Figure 4a that hollow microtubes with hexagonal structures were obtained, as well as self-assembled microrods in Figure 4b. Three different morphological structures can be marked on the images: Type 1: completely hollow hexagonal tubes; Type 2: partial filled hexagonal tubes; and Type 3: hexagonal rods (completely filled tubes), suggesting that each type of structure represents a phase of hexagonal microrods formation, as suggested in Figure 5.

Backscattered electron scanning image of fractured surface of composite resin modified by ZnO microstructures is showed in Figure 6. This image provided an adequate contrast between the resin matrix

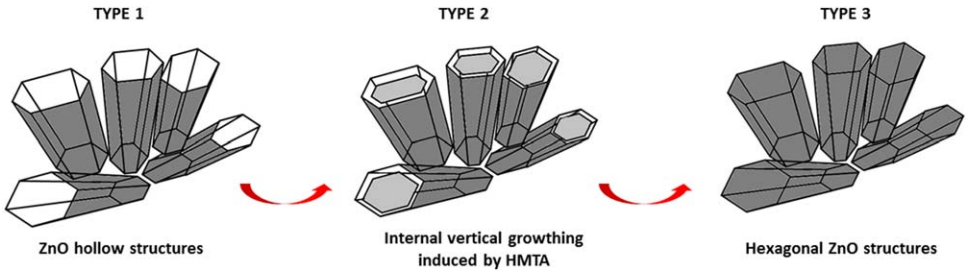

FIGURE 5 Self-assembly arrangement of hexagonal ZnO microstructures based on anisotropic growth. [Color figure can be viewed at wileyonlinelibrary.com]

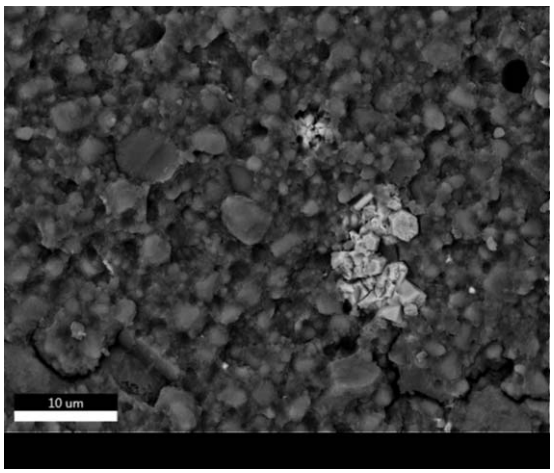

FIGURE 6 High resolution backscatter electron imaging of composite resin modified by ZnO, with field emission scanning electron microscopy

and fillers, which an agglomerated of ZnO rods can be clearly distinguished of organic matrix.

The chemical composition determined by EDX analysis of fractured surface of the restorative composite resin modified by ZnO microstructures, expressed in weight percentage are presented in Figure 7. The color mappings and spectra distinguished filler contents and provided their concentrations into composite resin matrix, detecting elements such as C, O Si, Zr, and Zn.

The MIC values of ZnO were found to be 125 μg/mL for *S. mutans*, 500 μg/mL for *C. albicans* and 62.5 μg/mL for *S. aureus*. In the tested concentrations, it was not possible to determine the MIC value against *E. coli*. The antimicrobial capacity of ZnO microstructures against *S. mutans*, *C. albicans*, *S. aureus*, and *E. coli* are demonstrated in terms of MIC values in Figure 8. Each point of the curves represents a concentration of ZnO suspension fold serial dilution.

Regarding antibacterial test of composite resin modified by ZnO, the results of bacterial colony count (Colony Forming Unit, CFU) after 24 hr of incubation are presented in Figure 9. Each column represents the mean values with standard deviation of counted CFU/mL for unmodified and modified composite resin in different concentrations. The first null hypotheses were rejected and the direct contact test demonstrates that the inclusion of 0.2, 0.5, and 1% in weight of ZnO on composite resin provided a statistical significant reduction ($p < 0.05$ for all cases) of colony formation units. Additionally, the increase of ZnO amount on resin leads to a decrease of CFU/mL.

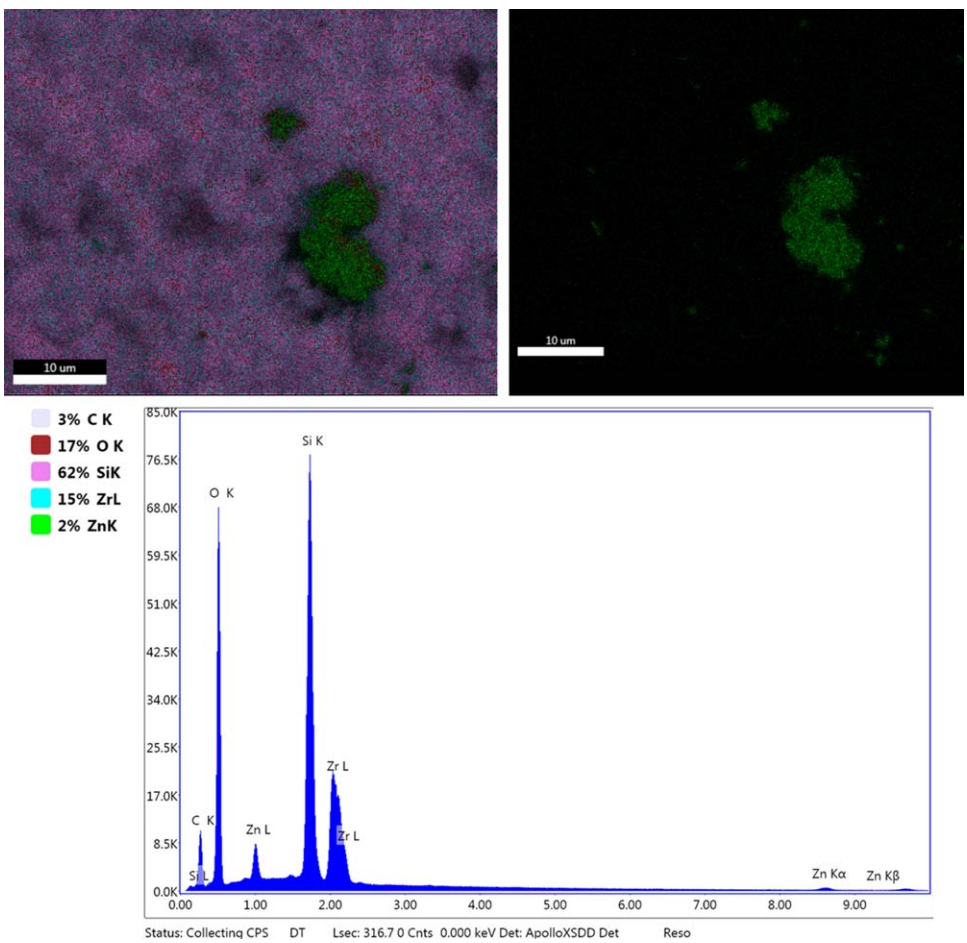

FIGURE 7 Energy dispersive X-ray spectra and color mappings of the fractured surface of the composite resin modified by ZnO microstructures as filler content. [Color figure can be viewed at wileyonlinelibrary.com]

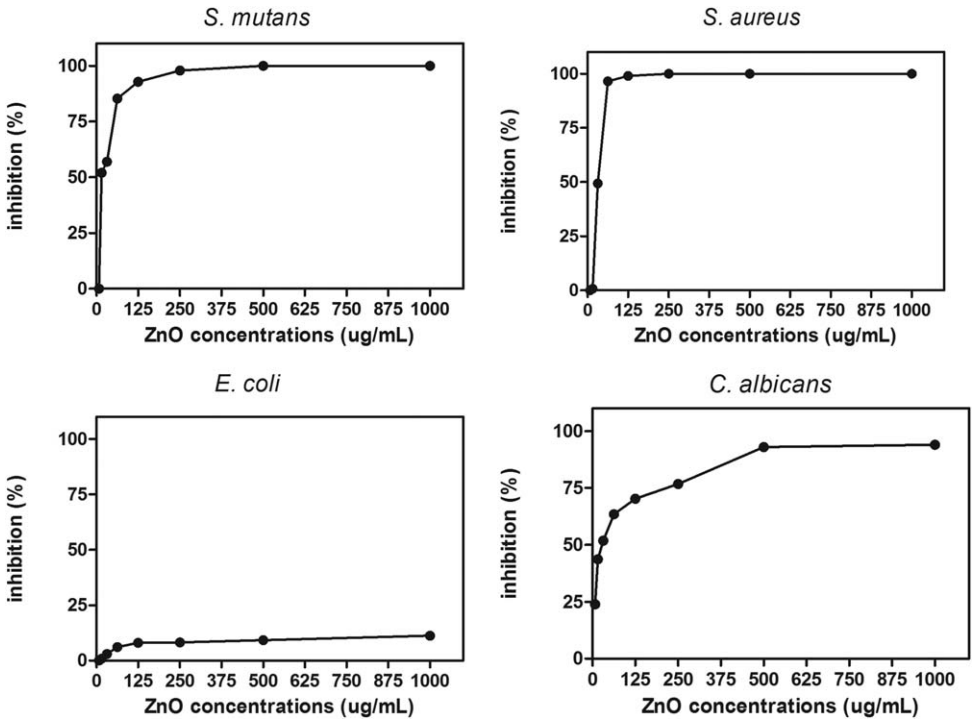

FIGURE 8 Antimicrobial inhibitory capacity of ZnO microstructures. The points of the curves represents concentrations of fold serial dilution

The mean and standard deviations values (MPa) for compressive strength and diametral tensile strength of unmodified and modified composite resin by ZnO microstructures (wt%) are shown in Figure 10. In this case, the second null hypothesis was accepted and the compressive strength of composite resin was not significantly affected ($p > 0.05$) after inclusion of ZnO microparticles. The inclusion of 0.5% and 1% in weight of ZnO significantly affected the diametral tensile strength of composite resin, but the modification with 0.2% of ZnO powder does not leads to significant differences in comparison to unmodified resin group.

4 | DISCUSSION

The hydrothermal approach was efficient to obtain crystalline ZnO in this study, allowing to the formation of ZnO with hollow and filled hexagonal rods microstructure. Considering the antibacterial effect of metal oxides particles, it is expected that the increasing in specific surface area of particles decrease the particle size decreases, allowing for greater material interaction with the surrounding environment and enhancing the extent of bacterial elimination (Seil & Webster, 2012). However, smallness itself is not the goal, besides surface area and particle size, different methods of synthesis in order to obtain novel physicochemical properties, such as particle shape and zeta potential, are also relevant variables affecting antibacterial activity (Pal, Tak, & Song, 2007; Seil & Webster, 2012). Zinc oxide have a broad spectrum antibacterial activity and presents, probably, the widest range of shapes in nanoscale, such as *nanowires*, *nanorods*, *nanobelts*, *nanopencils*, *nanosprings*, *nanocombs*, *nanoboxes*, and *nanorings* (Raghupathi, Koodali, & Manna, 2011; Sahu, Liu, Wang, & Kuo, 2015). ZnO morphology is determinate by synthesis method and conditions, which some parameters such as pH, temperature, solvents, precursor types, and physicochemical settings could be controlled in order to obtain structures for best antibacterial response (Sirelkhatim et al., 2015). It was demonstrated that the shape of ZnO could influence their mechanism of internalization, suggesting that rods and wires could penetrate into cell walls of bacteria more easily than spherical ZnO particles (Sirelkhatim et al., 2015; Yang, Liu, Yang, Zhang, & Xi, 2009). Regarding to this concept, particle surface properties possibly played a critical role in the reactive oxygen species production and the antibacterial activity of materials could be shape-dependent (Sirelkhatim et al., 2015; Yang, Liu,

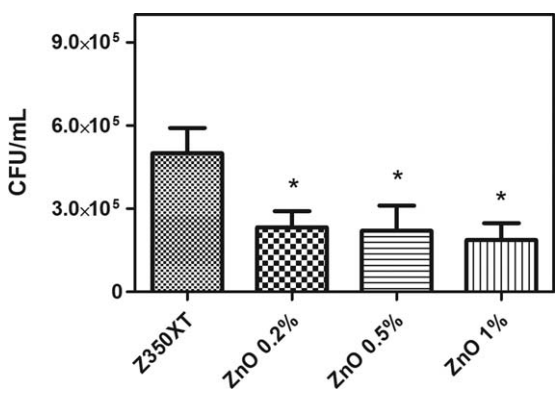

FIGURE 9 Colony forming unit (CFU/mL) following direct contact between *S. mutans* biofilm and composite resin modified by ZnO microstructures (% weight). *Indicate significant statistical differences in comparison to unmodified composite resin

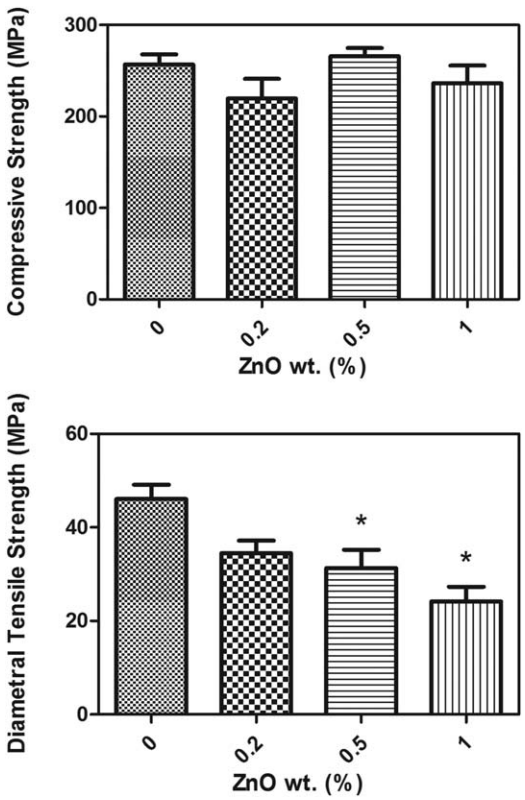

FIGURE 10 Compressive and diametral tensile strength of composite resin modified by ZnO microstructures (wt%). *Indicates significant statistical differences in comparison to unmodified composite resin.

Yang, Zhang, & Xi, 2009). The shape-dependent activity was explained in terms of the percent of active facets in the nanoparticles, which can be created as function of synthesis method and growth parameters. It has been demonstrated that rod-structures exhibit more active facets that leads to higher antibacterial activity in comparison to spherical nanostructures (Pal, Tak, & Song, 2007). In this study, we obtained microrods in two shapes, as demonstrated in SEM images in Figure 4. A plausible mechanism of formation and growth was proposed (Figure 5) in order to describe a hierarchical growth of ZnO structures. Based on a classical growth mechanism (Zhang et al., 2005), HMTA and zinc nitrate decompose into Zn^{2+} and OH^- ions. The ion concentration increases and ZnO nuclei are formed gradually during the hydrothermal process, due to the decomposition of a part of $Zn(OH)_2$ precipitates. HMTA induce formation of hexagonal crystal with central interface and produces hydroxide (OH^-) and NH_3 molecules in the solution. Certain $Zn(OH)_2$ precipitates are transformed into the growth units of $[Zn(OH)_4]^{2-}$ and $[Zn(NH_3)_4]^{2+}$ (Zhang et al., 2005). The anisotropic growth of rod-like structure and their formation from hollow rod-like structures depends on of adsorption of these units, determining the morphology of ZnO.

The chemical reactions involved in ZnO formation are (Jabeen, Iqbal, Kumar, Ahmed, & Javed, 2014):

$$Zn^{2+} + 4OH^- \rightarrow [Zn(OH)_4]^{2-} \quad (1)$$

$$Zn^{2+} + 4NH_3 \rightarrow [Zn(NH_3)_4]^{2+} \quad (2)$$

$$[Zn(NH_3)_4]^{2+} + 2OH^- \rightarrow ZnO + 4NH_3 + H_2O \quad (3)$$

$$[Zn(OH)_4]^{2-} \rightarrow ZnO + H_2O + 2OH^- \quad (4)$$

The rod size and dose were found as a determining parameter to achieve antibacterial activity [14]. Rago et al. (2014) investigated the antimicrobial capacity of ZnO microrods and nanorods against *S. aureus* and *Bacillus subtilis*. The authors related that nanorods demonstrated a superior antimicrobial effect in comparison to microrods. Wahab et al. (2012) reported high antibacterial activity of ZnO. They showed that microspheres solution inhibits the growth of microbial strain, which was found the inhibitory concentration of 5 μg/mL for *S. aureus*, *S. typhimurium*, and *K. pneumoniae* whereas for *E. coli*, it was found 15 μg/mL. Micro-flowers of ZnO were found to be an antibacterial agent when investigated against four pathogenic bacteria (*S. aureus*, *E. coli*, *S. typhimurium* and *K. pneumonia)* by taking five different concentrations (5–45 μg/mL), which 5 μg/mL inhibited the growth of microbial strain for all the tested pathogens (Wahab, Kim, Mishra, Yun, & Shin, 2010). A relevant antimicrobial activity was found to ZnO microrods against *E. coli*, *S. aureus*, and *S. mutans* in this study. In addition, it was noted activity against *C. albicans*, which shows the potential of ZnO in the inhibition of eukaryotic cells. The literature has shown that the use of nanoparticles, especially ZnO structures, against pathogenic microorganisms with high resistance pattern is proving to be a new source of research (Espitia et al., 2015). Our findings showed a possible selectivity of ZnO microstructures against Gram-positive cells, since that the ZnO have not shown a satisfactory inhibitory patterns against Gram-negative strain (*E. coli*). The study by Azam et al. (2012) showed the same selectivity pattern, since the activity of some compounds including ZnO nanoparticles, was superior in Gram-positive bacterial strains, including species used in this study. Jin, Sun, Su, Zhang, and Sue, (2009) reported the inhibitory potential of ZnO nanoparticles against *E. coli*, when it was used higher concentrations than used in this current study. The use of high concentrations could be not relevant, since this compound could exhibit greater toxicity. Since ZnO microstructures presents a high activity against *S. aureus*, such as found in this current work, this material could be an option to optimizing available antibiotics in the therapy of infections caused by this species, thereby generating a decrease in antimicrobial dose, toxicity and side effects (Thati, Roy, Prasad, Shivannavar, & Gaddad, 2010; Banoee et al., 2010).

The higher accumulation of dental plaque on the surface of restorative materials in comparison to enamel surface have determined a great interest towards new dental restorative materials containing antibacterial agents (Wang, Shen, & Haapasalo, 2014). Regarding antibacterial activity of composite resin modified by ZnO microrods, the results of this study show that small concentrations of self-assembled ZnO microrods and hollow microrods could inhibit bacterial and fungal strains. The incorporation into the composite resin allows to significantly inhibiting one of the major etiologic factors of caries formation, *S. mutans* biofilm accumulation, without alteration of tested mechanical properties of the resin. In agreement with our results, Kasraei et al. (2014) demonstrated a significant inhibition of *S. mutans* and

Lactobacillus in a composite resin containing ZnO nanoparticles. Sevinç and Hanley (2010) also demonstrated a resin blended by ZnO antibacterial capacity, which 10% (w/w) fraction of ZnO nanoparticles into dental composites displayed antimicrobial activity and reduced growth of bacterial biofilms by roughly 80% for a single-species model dental biofilm. Hojati et al. (2013) verified by direct contact test, a significant growth inhibition of *S. mutans* on the surface of a flowable composite resin containing 0–5 wt% nanoparticles of ZnO, without adversely changes of the mechanical properties of the composite at lower concentrations.

Regarding mechanical properties, the results of this study showed no statistical difference between unmodified and modified composite resin by ZnO, indicating that the addition of small amounts, such as 0.2%–1% in weight of ZnO, does not interfere in compressive and diametral tensile strength. The mechanical properties of nanofilled composite resins were considered as good as those of universal hybrids (Rastelli et al, 2012). Some studies investigated the use of different nano and microparticles in dental materials, including ZnO, concluding that the use of these particles in small concentrations does not interfere with the mechanical properties of the composite resin (Chen, Yu, Wang, & Li, 2011; Gjorgievska et al., 2015; Sevinç & Hanley, 2010).

Besides antibacterial activity, ZnO particles are opaque and their use in high concentrations can leads to greater opacity and lower the degree of conversion during polymerization (Hojati et al., 2013). On the other hand, the use of lower concentrations could provide a good dispersion into the composite resin, thereby increasing the compression strength (Chen, Yu, Wang, & Li, 2011; Sun et al., 2011). In summary, the mechanical properties are strongly influenced by polymerization, size, and amount of particles (Powers, 2006; Rastelli et al., 2012; Sun et al., 2011).

The controlled physical–chemical parameters to obtain ZnO microstructures can satisfactorily provide a better antibacterial activity of this material. It was demonstrated that microparticles could provide beneficial antibacterial properties on composite resins without alterations on its mechanical properties. The development of a new resin-based restorative material with these characteristics is desirable, which could contribute to reduce the occurrence of secondary caries. The results of this study demonstrated significant antimicrobial activity ZnO against *S. mutans*, *S.aureus*, and *C. albicans* strains. Additionally, the addition of 0.2%–1% in weight of ZnO microstructures into composite resin would significantly inhibit the growth of *S. mutans* on resin surface without significant alterations of its mechanical strength.

Based on our results, the modification of a composite resin with ZnO microparticles could be a good option to produce a novel antimicrobial restorative material. This novel material could be used in restorative dentistry instead of the traditional composite resins, reducing the bacterial accumulation over the restorations. ZnO microparticles could be also used as filler content in other restorative materials, such as flowable resins and glass ionomer cement. However, considering the limitations of this study, additional physical and mechanical tests could be performed in order to solve other possible remained questions.

ACKNOWLEDGMENTS

The authors would like to thank the Amazon State Research Foundation (FAPEAM, AM, Brazil) and Coordination for the Improvement of Higher Education Personnel (CAPES, Brazil) for the financial support for this investigation.

REFERENCES

Ajdic, D., McShan, W. M., McLaughlin, R. E., Savic, E., Chang, J., Carson, M. B., ... Ferretti, J. J. (2002). Genome sequence of *Streptococcus mutans* UA159, a cariogenic dental pathogen. *Proceedings of the National Academy of Sciences USA*, *99*, 14434–14439.

Alexander, L., & Klug, H. P. (1950). Determination of Crystallite Size with the X-Ray Spectrometer. *J Appl Phys*, *21*, 137–142.

American National Standard. (1993). American Dental Association Specification n. 27 for Resin-based filling materials,

Araújo, M. G. F., Hilário, F., Nogueira, L. G., Vilegas, W., Santos, L. C., Brunetti, I. L., ... Bauab, T. M. (2012). Correlation among antioxidant, antimicrobial, hemolytic, and antiproliferative properties of *Leiothrix spiralis* leaves extract. *International Journal of Molecular Sciences*, *13*, 9260–9277.

Araújo, M. G. F., Pacífico, M., Vilegas, W., Santos, L. C., Icely, P. A., Miró, M. S., ... Sotomayor, C. E. (2013). Evaluation of Syngonanthus nitens (Bong.) Ruhl. extract as antifungal and in treatment of vulvovaginal candidiasis. *Medical Mycology*, *51*, 73–682.

Azam, A., Ahmed, A. S., Oves, M., Khan, M. S., Habib, S. S., & Adnan, M. (2012). Antimicrobial activity of metal oxide nanoparticles against Gram-positive and Gram-negative bacteria: a comparative study. *International Journal of Nanomedicine*, *7*, 6003–6009.

Banoee, M., Seif, S., Nazari, Z. E., Jafari-Fesharaki, P., Shahverdi, H. R., Moballegh, A., & Shahverdi, A.,R. (2010). ZnO nanoparticles enhanced antibacterial activity of ciprofloxacin against *Staphylococcus aureus* and *Escherichia coli*. *Journal of Biomedical Materials Research B Applied Biomaterials*, *93*, 557–561.

Bonifácio, B. V., Ramos, M. A., da Silva, P. B., Negri, K. M., de Oliveira Lopes, E., de Souza, L. P., ... Bauab, T. M. (2015). Nanostructured lipid system as a strategy to improve the anti-Candida albicans activity of *Astronium* sp. *International Journal of Nanomedicine*, *10*, 5081–5092.

Burke, F. J., Crisp, R. J., Bell, T. J., Healy, A., Mark, B., McBirnie, R., & Osborne-Smith, K. L. (2001). One-year retrospective clinical evaluation of hybrid composite restorations placed in United Kingdom general practices. *Quintessence International*, *32*, 293–298.

Chen, L., Yu, Q., Wang, Y., & Li, H. (2011). BisGMA/TEGDMA dental composite containing high aspect-ratio hydroxyapatite nanofibers. *Dental Materials*, *27*, 1187–1195.

Corrêa, J. M., Mori, M., Sanches, H. L., da Cruz, A. D., Poiate Jr, E., & Poiate, I. A. V. P. (2015). Silver Nanoparticles in Dental Biomaterials. *International Journal of Biomaterials*, *2015*, 1–9.

CLSI, Manual Clinical and Laboratory Standards Institute. (2006). Methods for dilution antimicrobial susceptibility tests for bacteria that grow aerobically; approved standards – 6a ed. Document M7-A6 Performance Standards for Antimicrobial Susceptibility Testing. Clinical and Laboratory Standards Institute, Wayne, PA,

CLSI, Manual Clinical and Laboratory Standards Institute. (2008). Reference Methods for Broth Dilution Antifungal Susceptibility Tests for Yeasts; Approved Standards. CLSI document M27-A3. Wayne, PA,

Das Neves, P. B. A., Agnelli, J. A. M., Kurachi, C., & de Souza, C. W. O. (2014). Addition of silver nanoparticles to composite resin: Effect on physical and bacterial properties *in vitro*. *Brazilian Dental Journal*, *25*, 141–145.

Espitia, P. J. P., Soares, N. F. F., Coimbra, J. S. R., de Andrade, N. J., Cruz, R. S., & Medeiros, E. A. A. (2015). Zinc oxide nanoparticles: synthesis, antimicrobial activity and food packaging applications. *Food and Bioprocess Techonoly*, *5*, 1447–1464.

Gjorgievska, E., Tendeloo, G. V., Nicholson, J. W., Coleman, N. J., Slipper, L. J., & Booth, S. (2015). The incorporation of nanoparticles into conventional glass-ionomer dental restorative cements. *Microscopy and Microanalysis*, *21*, 392–406.

Gudiña, E. J., Rocha, V., Teixeira, J. A., & Rodrigues, I. R. (2010). Antimicrobial and antiadhesive properties of a biosurfactant isolated from *Lactobacillus paracasei* ssp. Paracasei A20. *Letters in Applied Microbiology*, *50*, 419–424.

Hojati, S. T., Alaghemand, H., Hamze, F., Babaki, F. A., Rajab-Nia, R., Rezvani, M. B., … Atai, M. (2013). Antibacterial, physical and mechanical properties of flowable composite resins containing zinc oxide nanoparticles. *Dental Materials*, *29*, 495–505.

Jabeen, M., Iqbal, M. A., Kumar, R. V., Ahmed, M., & Javed, M. T. (2014). Chemical synthesis of zinc oxide nanorods for enhanced hydrogen gas sensing. *Chinese Physics B*, *23*, 1–4.

Jin, T., Sun, D., Su, J. Y., Zhang, H., & Sue, H. J. (2009). Antimicrobial efficacy of zinc oxide quantum dots against *Listeria monocytogenes*, *Salmonella Enteritidis*, and *Escherichia coli* O157:H7. *Journal of Food Science*, *74*, M46–M52.

Kasraei, S., Sami, L., Hendi, S., AliKhani, M. Y., Rezaei-Soufi, L., & Khamverd, Z. (2014). Antibacterial properties of composite resins incorporating silver and zinc oxide nanoparticles on *Streptococcus mutans* and *Lactobacillus*. *Restorative Dentistry and Endodontics*, *39*, 109–114.

Pal, S., Tak, Y. K., & Song, J. M. (2007). Does the antibacterial activity of silver nanoparticles depend on the shape of the nanoparticle? a study of the Gram-negative bacterium *Escherichia coli*. *Applied Environmental Microbiology*, *73*, 1712–1720.

Powers, J. M. (2006). *Restorative dental materials*. St. Louis: Mosby.

Raghupathi, K. R., Koodali, R. T., & Manna, A. C. (2011). Size-dependent bacterial growth inhibition and mechanism of antibacterial activity of zinc oxide nanoparticles. *Langmuir*, *27*, 4020–4028.

Rago, I., Chandraiahgari, C. R., Bracciale, M. P., De Bellis, G., Zanni, E., Guidi, M. C., … Uccelletti, D. (2014). Zinc oxide microrods and nanorods: different antibacterial activity and their mode of action against Gram-positive bacteria. *RSC Advances*, *4*, 56031–56040.

Rastelli, A. N. S., Jacomassi, D. P., Faloni, A. P. S., Queiroz, T. P., Seila, S. R., Bernardi, M. I. B., … Hernandes, A. C. (2012). The filler content of the dental composite resins and their influence on different properties. *Microscopy Research Technique*, *75*, 758–765.

Sahu, D. R., Liu, C. P., Wang, R. C., & Kuo, C. L. (2015). Growth and application of ZnO nanostructures. *International Journal of Applied Ceramamic Technology*, *10*, 814–838.

Sakaguchi, R. L. (2005). Review of the current status and challenges for dental posterior restorative composites: clinical, chemistry, and physical behavior considerations. *Dental Materials*, *21*, 3–6.

Seil, J. T., & Webster, T. J. (2012). Antimicrobial applications of nanotechnology: methods and literature. *International Journal of Nanomedicine*, *7*, 2767–2781.

Sevinç, B. A., & Hanley, L. (2010). Antibacterial activity of dental composites containing zinc oxide nanoparticles. *Journal of Biomedical Materials Research B Applied Biomaterials*, *94*, 22–31.

Sirelkhatim, A., Mahmud, S., Seeni, A., Kaus, N. H. M., Ann, L. C., Bakhori, S. K. M., … Mohamad, D. (2015). Review on zinc oxide nanoparticles: antibacterial activity and toxicity mechanism. *Nano-Micro Letters*, *7*, 219–242.

Sun, J., Forster, A. M., Johnson, P. M., Eidelman, N., Quinn, G., Schumacher, G., … Wu, W. L. (2011). Improving performance of dental resins by adding titanium dioxide nanoparticles. *Dental Materials*, *27*, 972–982.

Thati, V., Roy, A. S., Prasad, M. V. N. A., Shivannavar, C. T., & Gaddad, S. M. (2010). Nanostructured zinc oxide enhances the activity of antibiotics against *Staphylococcus aureus*. *Journal of Bioscience and Technology*, *1*, 64-–69.

Wahab, R., Kim, Y. S., Mishra, A., Yun, S. I., & Shin, H. S. (2010). Formation of ZnO micro-flowers prepared via solution process and their antibacterial activity. *Nanoscale Research Letters*, *5*, 1675–1681.

Wahab, R., Mishra, A., Yun, S. I., Hwang, I. H., Mussarat, J., Al-Khedhairy, A. A., … Shin, H. S. (2012). Fabrication, growth mechanism and antibacterial activity of ZnO micro-spheres prepared via solution process. *Biomass & Bioenergy*, *39*, 227– 236.

Wang, Z., Shen, Y., & Haapasalo, M. (2014). Dental materials with antibiofilm properties. Dental. *Materials*, *30*, e1–e16.

Yang, H., Liu, C., Yang, D., Zhang, H., & Xi, Z. (2009). Comparative study of cytotoxicity, oxidative stress and genotoxicity induced by four typical nanomaterials: the role of particle size, shape and composition. *Journal of Applied Toxicology*, *29*, 69–78.

Zhang, H., Yang, D., Li, D., Ma, X., Li, S., & Que, D. (2005). Controllable growth of ZnO microcrystals by a capping-molecule-assisted hydrothermal process. *Crystal Growth & Design*, *5*, 547–550.

How to cite this article: Dias HB, Bernardi MIB, Ramos MAS, et al. Zinc oxide 3D microstructures as an antimicrobial filler content for composite resins. *Microsc Res Tech*. 2017;80:634–643. https://doi.org/10.1002/jemt.22840